RAPID DETERMINATION OF FATIGUE LIMIT OF COMPOSITES BY LUONG'S METHOD AND ITS IMPROVEMENT

Jia Huang[1], Marie-Laetitia Pastor[1], Christian Garnier[2], Xiaojing Gong[1]

[1] Univ. Toulouse, IUT Tarbes, ICA, 1 rue Lautréamont F-65016 Tarbes, France
[2] Univ. Toulouse, INP-ENIT, LGP, 47 avenue d'Azereix, F-65016 Tarbes, France

Keywords: Composite laminates, fatigue limit, infrared thermography

ABSTRACT

Composite materials are widely used in structures which are subjected to cyclic loading, such as airframe and turbine blades. In structure design, the fatigue performance needs to be taken into account to ensure structural integrity. The traditional fatigue testing usually is time consuming and costly. Luong's method, which is based on infrared thermographic data analysis, has been proven to be rapid and efficient for fatigue limit determination in metallic materials. It has also been considered for composites. However, the procedure of Luong's method involves visual inspection which leads to man-made uncertainties. In the present paper, improved thermographic data analysis methods are proposed to determine the fatigue limit with uniqueness. The first method divides the original experimental data into two parts by estimating the maximum turning point in the curve of the temperature response as a function of the applied stress amplitude. The second method aims to characterize relationship between applied stress amplitude and temperature response using a consistent formula. The fatigue limit can be identified by the minimum curvature radius of the curve. The last method is based on the goodness of fitting as in statistical analysis. With the consideration of both the intersection position and the goodness of linear fitting, the fatigue limit can be calculated. A MATLAB© program is developed for this purpose. All three improved methods are examined with experimental data in literature.

1 INTRODUCTION

Composite materials are increasingly used in an ever-wider applications due to their high strength-to-weight ratio, easy formability and other properties. Composites are commonly used in high cycle fatigue applications including ship hull, aircraft, and wind turbine blade structures [1, 2]. The fatigue limit, a key property of the dynamic performance of a material, is conventionally determined using the '*S-N* curve' approach [3] and standard staircase method [4]. The traditional fatigue characterization methods require testing a large number of specimens at different load levels [5]. It is time-consuming and costly but indispensable for product design in industry. As for composites, the diversity is richer than metals. It is a formidable task to use the traditional methods to optimize fiber proportion and ply scheme of composites.

The thermographic method has been widely used in engineering applications. Based on the curve of stabilized temperature in the specimen as a function of the applied stress amplitude, Luong et al. proposed to identify the fatigue limit by finding the point when a drastic change in the rate of intrinsic dissipation happens [6-9]. This is done by interpolating the experimental data by two lines, one for stresses below and the other for stresses above the fatigue limit. Besides metallic materials, Luong's method has also been used in composite materials [10-17]. The literature indicates that Luong's method makes it possible to acquire fatigue limit within a short time and can be used for almost any stress ratio. Unfortunately, the procedures of graphic fatigue limit determination are controversial and questionable: How to choose the proper points to fit the lines with uniqueness? Why should we use straight lines to fit the data, not other kind of curves? The physical mechanism is not yet well understood. Thus, an optimization of Luong's methods and a better understanding of the correlation between the level of loading stress and temperature response is required in order to better interpret experimental results.

In the present paper, we developed new treatment methods of experimental data so as to determine the fatigue limit of composites with uniqueness. Three improved methods were developed and applied to the experimental data found in the literature. In addition, the error analysis for these three methods has been carried out. The results are compared.

2 BACKGROUND OF INFRARED THERMOGRAPHY

It is a common phenomenon that the plastic deformation and damage accumulation in specimen are accompanied by the generation of a large amount of heat. This inspires researchers to measure the temperature change as an effective approach of studying fatigue behaviour. The fatigue-related temperature rise and heat emission of both metal and composite were studied as early as in the 1970s [18] and [19]. Meanwhile, the scanning infrared camera was used to visualize the surface-temperature field [20]. During fatigue tests, the following coupled thermomechanical equation was employed [7]:

$$\rho C_{\mathrm{v}} \dot{T} = r_0 + K \nabla^2 T - \left(\beta : \overset{4}{D} : \dot{E}^e \right) T + S : \dot{E}^I \tag{1}$$

where the volumetric heat capacity $C = \rho C_v$ of the material is the energy required to raise the temperature of a unit volume by 1 ℃, C_v is the specific heat at constant deformation , T is the absolute temperature, K is the thermal conductivity, β is the coefficient of the thermal expansion matrix, $\overset{4}{D}$ is the fourth-order elasticity tensor, E^e the elastic strain tensor, E^I is the inelastic strain tensor and S is the specific entropy. There are four terms on the right-hand side of the thermomechanical equation above. Heat sources, the first term, is due to sources or sinks of heat in the scanning field. Thermal conduction, the second term, governs the transfer of heat by conduction which leads to a uniform temperature on the specimen. Thermo-elasticity, the third term, illustrates the thermos-elastic coupling effect. Intrinsic dissipation, the last term, defines the energy dissipation due to plasticity and viscosity (irreversible degradation). In this paper, the external heat sources are considered as time-independent, the thermal conduction is dependent on material constants, and the thermos-elasticity has no influence on mean temperature rising [21]. Thus, the stabilized shift can be considered as the consequence of intrinsic dissipation.

In composites laminates, the damage process observed under fatigue loading can be divided into three main stages: (I) rapid growth, (II) leveling-off and (III) rapid damage accumulation, see Figure 1. The same three stages can be distinguished during evolution of the temperature rising which is a consequence of the intrinsic dissipation due to damage, as shown in Figure 2. Especially during stage (II), the temperature rising remains stable and with the increasing of loading amplitude (σ_a), the stabilized temperature shifting (T_{rstab}) is rising.

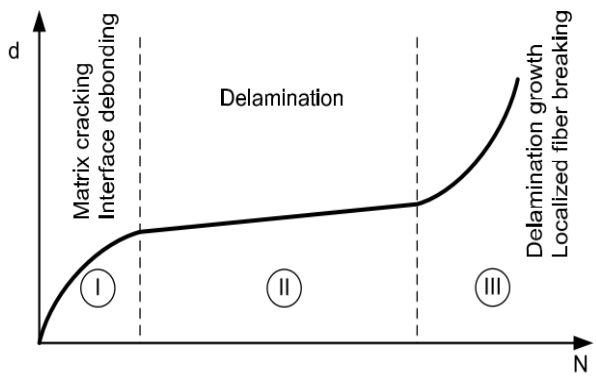

Figure 1: Damage accumulation within cycles [22].

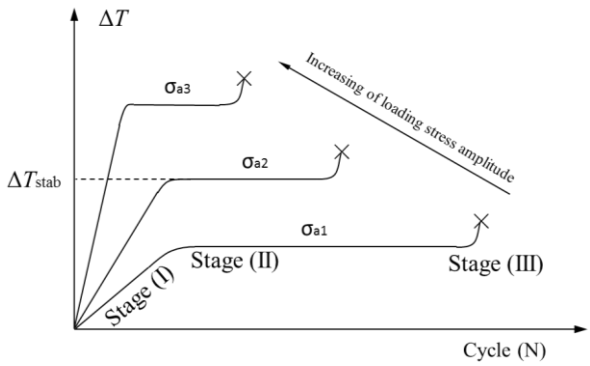

Figure 2: Observed temperature evolution during constant amplitude fatigue tests

Since it is not necessary to run the fatigue test until specimen failures to acquire the value of stable increased temperature, the stepped loading pattern is adopted. After a certain number of load cycles, the stable value of temperature rising is recorded. Increasing the loading stress amplitude and repeating the process above, the correlation of T_{rstab} and stress amplitude σ_a can be obtained, as illustrated in Figure 3. During the whole test, the stress ratio is kept constant. Luong's method utilizes one straight line to characterize thermo-elastic effect and another straight line to describe temperature rising when thermoplastic effect becomes dominant. By finding a drastic change in the rate of intrinsic dissipation, the fatigue limit can be evaluated in a very short time. Figure 3 shows the determination process of Luong's method. The intersection of two straight lines is considered as the fatigue limit.

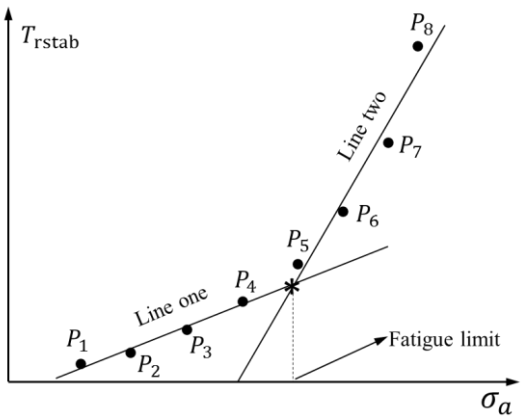

Figure 3: Determination of fatigue limit by Luong's method

Unfortunately, Luong's method does not have a strict standard to divide the data into two sets of point. A common way is to find a dramatic change in the loci of T_{rstab} versus σ_a manually and separate the points into two groups. This process is usually visual and contains artificial uncertainties. Different individuals may obtain distinct fatigue limit according to same experimental data. In addition, most data founded on the literature are based on temperature instead of intrinsic dissipation even if it is the most phenomenological approach. Therefore, in order to determine the fatigue limit with uniqueness, three new methods, based on temperature, are proposed for the treatment of experimental data.

3 DESCRIPTION OF NEWLY DEVELOPED TREATMENT METHODS

Three methods are developed for this analysis. There are termed as Method I, II, and III thereafter. Method I is based on the determination of the turning point in experimental data that allows dividing the original data into two groups. Herein, the peak value of the angle change is considered as the turning point. And then linear regression of the points in each group gives the fatigue limit according to Luong's method. Method II uses a consistent curve to characterize the loci of the stabilized temperature rising versus applied stress amplitude. The temperature response of low applied stress amplitude is similar as the first linear line of Luong's method, whereas the temperature rising for high applied stress is nearly exponential. The minimum radius of curvature of the fitted function indicates the turning point of the curve and can be considered as the fatigue limit. Method III is based on goodness of fitting. All the possibility of separating situation for original data will be calculated and Luong's method will be applied. With the consideration of both intersection position and goodness of linear fitting, the fatigue limit will be chosen by using MATLAB© program without human intervention.

3.1 Method I

If Luong's method is used to determine the fatigue limit, the question is how to find correctly the point that separates all experimental data into two groups. According to the hypothesis of Luong's

method, the line of small slope (Line one) is used to characterize the temperature response of stress amplitude below fatigue limit and the line of large slope (Line two) is used to describe the temperature response of stress amplitude above fatigue limit, as illustrated in Figure 3. Thus, we can deduce that if the points used for fitting Line one are all below fatigue limit, the slope of linear fitting is relatively similar, and if we take some points which are above fatigue limit into linear fit of Line one, the slope may change dramatically. And the same deduction is also suitable for Line two. Noticed that Luong's method is a graphic method and the relationship of slope versus the angle (θ) formed by the Line one and the x-axis (σ_a) is not linear, it is better to use angle change instead of slope change.

In order to characterize the angle change, a normalized angle is used. The points on figure 3 are numbered as $P_1, P_2, P_3 \dots P_n$ and n is the total number of points. Thus, the definition is shown as follows:

$$\theta_i^c = \left| \frac{\theta_{i+1} - \theta_i}{\max(\theta_{2,3,4\dots}) - \min(\theta_{2,3,4\dots})} \right| \ (\mathrm{i} \geq 2) \tag{2}$$

where the subscript i represents the sequence number of the points, as shown in Figure 3. θ_i is the angle between x-axis (σ_a) and the line determined by point-set $\{P_{i-1}, P_i\}$, as illustrated in Figure 4. The term $\max(\theta_{2,3,4\dots}) - \min(\theta_{2,3,4\dots})$ is used to normalize angle change. θ_i^c is the normalized angle change between line fitted by point-set $\{P_{i-1}, P_i\}$ and point-set $\{P_i, P_{i+1}\}$.

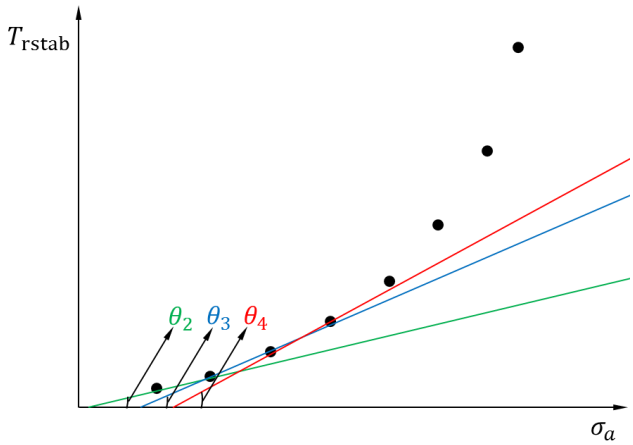

Figure 4: Schematic definition of θ_i

Figure 5 gives a typical distribution of θ_i^c obtained by applying this method to the data from [16].

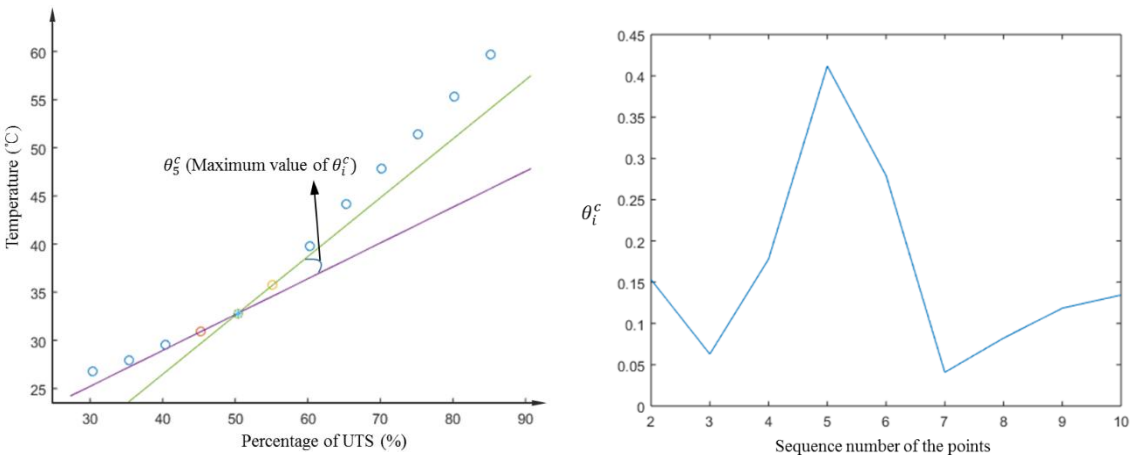

(a) (b)

Figure 5: A typical distribution of θ_i^c. (a) Original experimental data from [16]. (b) Loci of θ_i^c versus sequence number of point

As can be seen from Figure 5, if the experimental data shows a good bilinear behavior, we can easily find a peak value of θ_i^c, which means the angle changes dramatically at this point. Thus, the data can be separated into two groups by the peak node, and then Luong's method can be used to determine the fatigue limit. If the experimental data contain too much fluctuation, this method fails to produce a correct value.

3.2 Method II

As it is well known, Luong et al. used two straight lines to characterize the loci of $\mathrm{T_{rstab}}$ versus σ_a. Thus, the gradient, $\Delta T_{\mathrm{rstab}}/\Delta\sigma_a$, highlights a sudden change before and after the fatigue limit, which may not meet the common physical facts. Therefore, we try to characterize T_{rstab} versus σ_a data using a consistent curve, so the minimum curvature radius of curve may indicate the dramatic turning point of T_{rstab}, as shown in Figure 6.

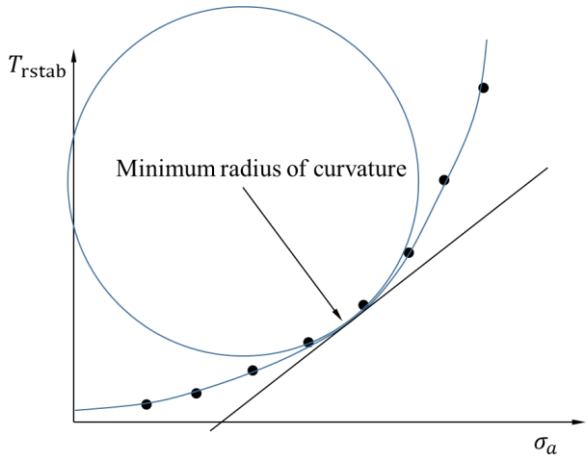

Figure 6: Schematic definition of minimum curvature radius

A three-parameter function was developed to characterize the curve by fitting. The expression is established as follows:

$$T_{\mathrm{rstab}} = a \cdot \exp\left(b\sigma_a - \frac{1}{b\sigma_a}\right) + c\sigma_a \tag{3}$$

where the first term on right side is used to describe the temperature response under high loading stress amplitude, and the second term on the right side is used to represent the temperature rising under low loading stress amplitudes. a, b, c are three parameters of interpolation to be determined. a is used to regulate the amplitude of exponential function, b is used to adjust σ_a axis range, and c is used to describe the amplitude of temperature rising in low stress cases. Thus, under the situation of low σ_a, the curve of Eq. (3) is similar to Line one, whereas, when σ_a becomes high enough, the curve of the expression is near to Line two of Luong's method. The calculation formula of curvature radius is given as follow:

$$R_\rho = \frac{1}{\kappa} = \left|\frac{(1+\dot{y})^{\frac{3}{2}}}{\ddot{y}^2}\right| \tag{4}$$

where $\dot{y} = \mathrm{d}\,T_{\mathrm{rstab}}/\mathrm{d}\sigma_a$, $\ddot{y} = \mathrm{d}^2 T_{\mathrm{rstab}}/\mathrm{d}^2\sigma_a$, κ the curvature, and R_ρ curvature radius. We apply this model to experimental data from literature [10], and a typical result is shown in Figure 7.

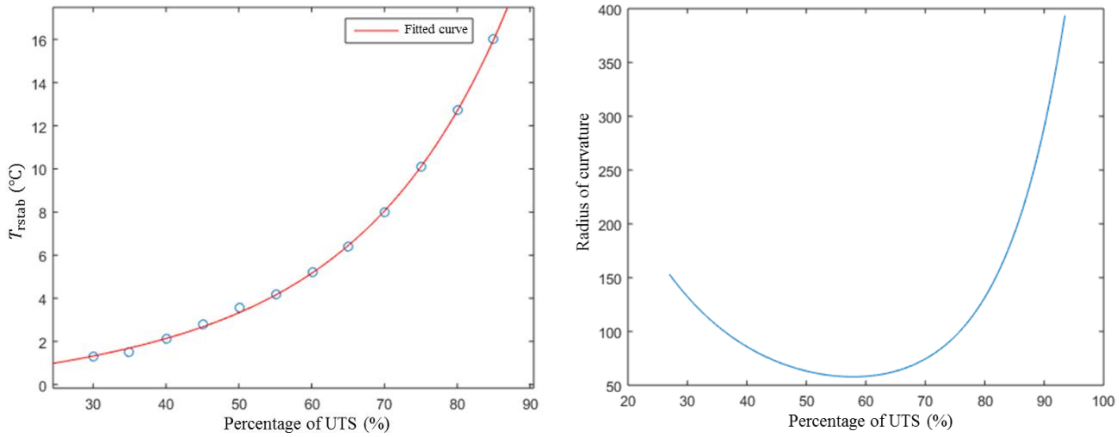

(a) (b)

Figure 7: A typical result of Method two. (a) The curve fitted by adopting Eq. (5) (data from [10]). (b) The loci of curvature radius versus percentage of ultimate tension stress (UTS)

As can be seen from Figure 7, the fitted curve matched well with the experimental data and the corresponding loci of curvature radius versus UTS can be accordingly determined. The minimum curvature radius indicates the most dramatic changing point and we naturally identified the related applied stress amplitude as the fatigue limit. The detailed results are shown in Table 1.

3.3 Method III

This method is inspired from the iterative approach proposed by F. Curà et al. [23]. The specific procedure of their method is held as follows:

(1) Choose a 'first trial stress' σ_{t1}, and split the data into two groups below (Group one) and above (Group two) the value of σ_{t1}, respectively.

(2) Two different curves (straight lines) are then utilized to interpolate experimental points in those two groups and obtain the intersection as 'second trial stress', the error is defined as $\sigma_{ti} - \sigma_{t(i-1)}$.

(3) Increase (decrease) the trial stress if the error is positive (negative).

(4) The procedure stops when the error is less than a prefixed value.

However, for a number of experimental results, this iterative approach may not work properly. The author did not provide the step length of increasing or decreasing in step (3) and specify how to choose a prefixed value in the published paper. Anyway, we can set the step length as variable equalling to the error in step (4) and the prefixed error value is 0. After applying this method to the experimental data from [24], the results are shown in Figure 8.

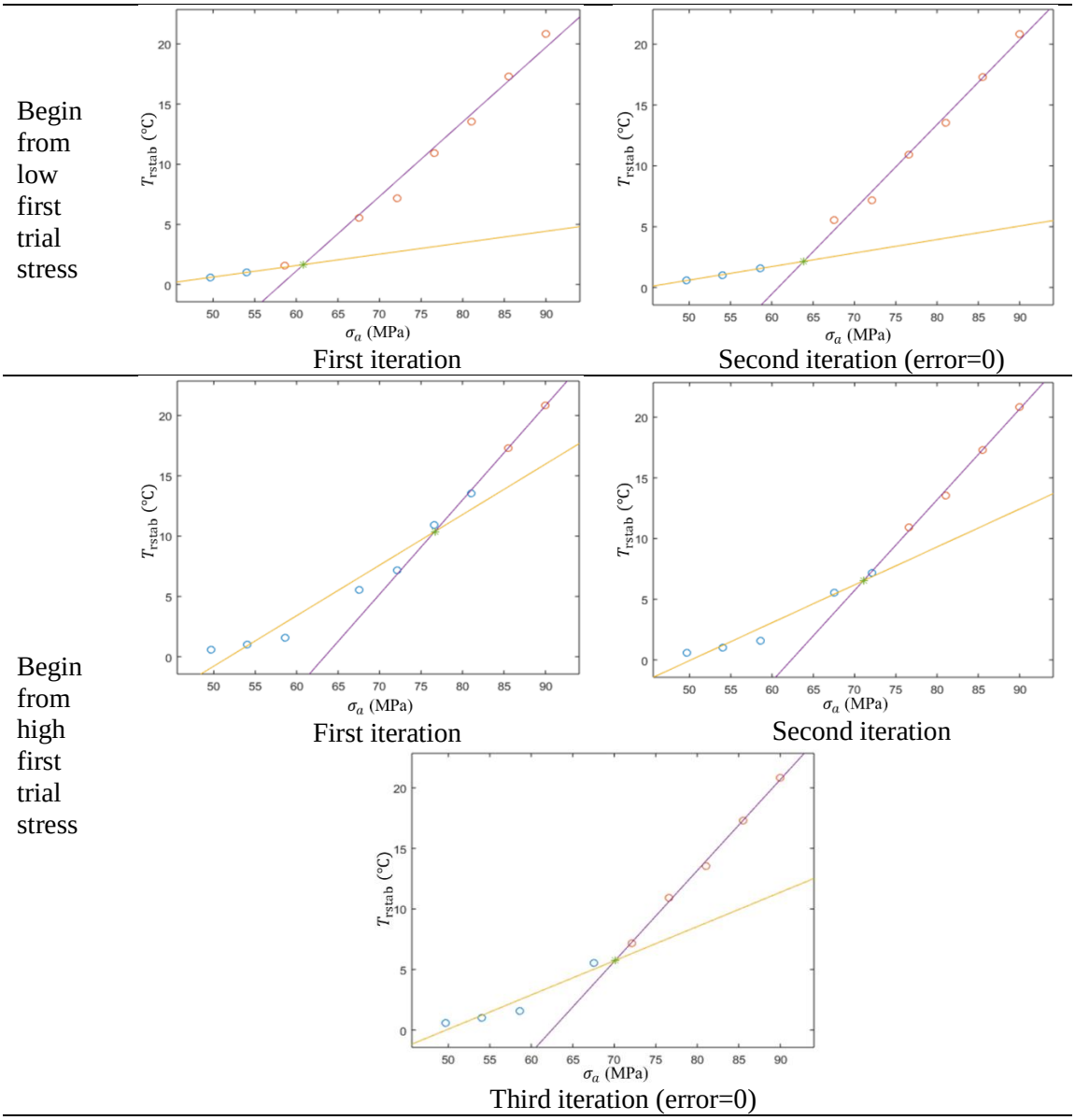

Figure 8: The specific procedure of iteration from low and high first trial stress (data from [24])

As shown in Figure 8, if the first trial stress is chosen at a low level, after two iterations, the error is 0, whereas, for high first trial stress, after three times iterations the error is 0 as well. However, the determined fatigue limits are not the same value. So we cannot have a unique answer. In fact, for most cases, we still need to decide which one is the proper fatigue limit empirically. Here, we propose a method based on statistical analysis. If two lines can well characterize the temperature rising versus stress amplitude, the goodness of fit is expected to be high. Commonly we use R^2 to evaluate the goodness of fit. The formula is expressed as:

$$R^2 = \frac{\left[\sum(X_i - \bar{X})\sum(Y_i - \bar{Y})\right]^2}{\sum(X_i - \bar{X})^2 \sum(Y_i - \bar{Y})^2} \tag{5}$$

where X_i is x-coordinate and Y_i is y-coordinate. $\bar{X}$ and $\bar{Y}$ is the mean value of X_i and Y_i, respectively. Herein, the goodness of two lines is defined as:

$$R_T{}^2 = (R_1{}^2 + R_2{}^2)/2 \tag{6}$$

where R_1 is the fitting goodness of Line one and R_2 is the fitting goodness of Line two. The combinations of point-sets are expressed as $\{P_1, P_2, \dots P_k\}$ and $\{P_{k+1}, P_{k+2}, \dots P_n\}$, where k is split point number and $2 \le k \le n-1$. We apply Luong's method to all the possible combinations and the results

are shown in Figure 9.

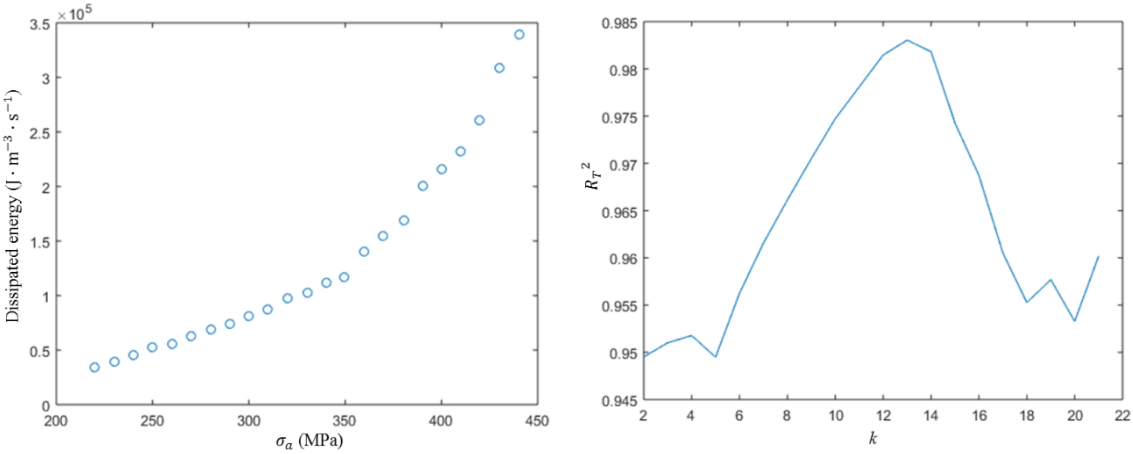

(a) (b)

Figure 9: Goodness of fit versus the sequence number of separated point. (a) Original experimental data from [25]. (b) Curve of $R_T{}^2$ versus split point number k

As can be seen from Figure 9, the value of $R_T{}^2$ follows a trend of increase-highest-decrease in the whole process. The high values of $R_T{}^2$ indicate the both lines can be well fitted by the experimental data. Meanwhile, it should also be noticed that the stress amplitude σ_a corresponding to points which used to fit Line one should be lower than the determined fatigue limit while the stress amplitude of points related to Line two should be higher than fatigue limit. After excluding the combinations of point-sets which do not meet the condition mentioned above, the intersection of the two lines with the best goodness of fit can be considered as the fatigue limit. MATLAB© is employed here and the procedure of this method is summarized as follows:

(1) List all the possible combinations of two point-sets, such as $\{P_1, P_2, \dots P_k\}$ and $\{P_{k+1}, P_{k+2}, \dots P_n\}$, from original data according to split point number k;

(2) The experimental points in those point-sets will be interpolated by two different laws (linear law here) to obtain the intersection point P_i;

(3) Choose all the split combinations of two groups if $\sigma_{P_k} \leq \sigma_{P_i} \leq \sigma_{P_{k+1}}$, where σ_{P_k}, σ_{P_i} and $\sigma_{P_{k+1}}$ are the stress amplitude corresponding to points P_k, P_i and P_{k+1}, respectively (This idea is given by F. Curà et al. [23]);

(4) Apply the goodness check (calculate $R_T{}^2$) and choose the combination with best goodness of fit, so the stress amplitude of intersection point P_i obtained from this combination is fatigue limit.

5 RESULTS AND DISCUSSION

For comparison, Table 1 lists the results of fatigue limit from the literature, based on temperature, obtained from manual graphic method and conventional experimental method. These experimental data are also used to determine the fatigue limit by applying the three methods proposed in this paper. It is noted that except for the data in grayscale shade, the results obtained by three proposed methods in general agree well with those from the literature using the manual graphic method and conventional experimental measurement. However, there are also some drawbacks and limits in application of each method presented here.

As for Method one, the results obtained for some cases are pretty good, especially for the cases where the rising of the temperature is monotone with the applied stress amplitude, such as the data from literature [16]. But it does not work well for all experimental data. If the curve of temperature rise contains some fluctuations, the precision of the Method one can be significantly perturbed. As demonstrated in Table 1, the relative error is important when Method one is applied to the data from references [13] and [17]. Method two can be applied to most of the experimental results and the error of predicted fatigue limit is acceptable for all experimental data. Put it into details, the predicted value is always smaller than the experimental results, especially the results of reference [13] and [17]. It

confers to this method a conservative power. The minimum curvature radius characterizes the turning point of the curve, which indicates that the dissipated energy starts to increase more and more rapidly. There are also some drawbacks. The data used for fitting need to have a wide range of applied stress amplitudes and enough points (usually more than 8) to ensure the stability of undetermined parameters. For Method three, generally speaking, its scope of applications is the widest and the error is also relatively smaller. For the fatigue data in [13], the precision of Method three is better than manual graphic method. It is suitable for almost all the data from literature. Comparing the results obtained by Method three with those from traditional methods, the relative error is less than 8% for all data presented in this paper (see Table 1).

5 CONCLUSIONS

In this work, three new methods are developed in determination process of fatigue limit of material based on the measurement of temperature rise as a function of the applied stress amplitude using an infrared camera. The aim is to obtain the fatigue limit with uniqueness by using the graphic method for the rapid evaluation of fatigue limit based on thermographic data analysis. These treatment methods of experimental data are applied to a large number of experimental data found in the literature to test their efficiency and their limit. It is shown that Method one, based on the maximum angle change, it can be successfully applied on the data where a monotone temperature increasing is observed as a function of the applied stress amplitude. Unfortunately, this method fails if the temperature varies with the stress amplitude in a zigzag way. For Method two, an exponential function is developed to describe the loci of T_{rstab} versus σ_a. The fatigue limit can be determined by the point having minimum curvature radius. The values of fatigue limit are usually less than that from classical experimental measurements, so it is a conservative method. A wide range of loci of T_{rstab} versus σ_a is necessary for adopting this method. Method three combines goodness of two linear laws fitting and Luong's method. This method has been applied successfully to almost all the data from literature used in this study. The relative error is less than 8%.

ACKNOWLEDGEMENTS

The author Jia Huang was supported by the China Scholarship Council for 3 years study at the University of Toulouse.

No.	Geometry	Material	Unit	Graphic method in Rf. (GM)	Traditional Experiments in Rf. (TE)	Method 1 (M1)	Method 2 (M2)	Method 3 (M3)	$\frac{M1-GM}{GM}$	$\frac{M1-TE}{TE}$	$\frac{M2-GM}{GM}$	$\frac{M2-TE}{TE}$	$\frac{M3-GM}{GM}$	$\frac{M3-TE}{TE}$
[13]	±45° Flat	carbon/epoxy Fabric	UTS	0.50	0.53	0.68	0.47	0.52	36.07%	28.37%	-5.40%	-10.75%	3.52%	-2.34%
[10]	flat	CFRP Woven	UTS	0.64	0.63	0.67	0.58	0.67	5.17%	7.69%	-9.63%	-7.46%	5.17%	7.69%
[16]	0° Flat	CFRP	UTS	0.51	0.53	0.51	0.52	0.50	0.78%	-2.10%	2.52%	-0.40%	-1.61%	-4.42%
[17]	0° Flat	CFRP (test 1)	MPa	390	400	346.75	362.24	382.99	-11.09%	-13.31%	-7.12%	-9.44%	-1.80%	-4.25%
[17]	0° Flat	CFRP (test 2)	MPa	390	400	311.57	372.18	380.62	-20.11%	-22.11%	-4.57%	-6.95%	-2.41%	-4.85%
[12]	±45° Flat	GFRP	MPa	36	Null	37.57	33.97	37.57	4.35%	Null	-5.65%	Null	4.35%	Null

Table 1: Summarized results of fatigue limit obtained from manual graphic method, conventional experimental method and Method 1, 2, 3. (UTS is Ultimate Tension Stress for composites. Null: no available values. Failed: the method failed to generate an answer for fatigue limit)

REFERENCES

[1] C.W. Kensche, Fatigue of composites for wind turbines. *International journal of fatigue*, **28**(10), 2006, pp. 1363-1374.

[2] P.H. Shin, S.C. Webb and K.J. Peters, Pulsed phase thermography imaging of fatigue-loaded composite adhesively bonded joints. *NDT & E International*, **79**, 2016, pp. 7-16.

[3] F.G. Pascual and W.Q. Meeker, Estimating fatigue curves with the random fatigue-limit model. *Technometrics*, **41**(4), 1999, pp. 277-289.

[4] J. Braam and S. Van der Zwaag, A statistical evaluation of the staircase and the arcsin√ P methods for determining the fatigue limit. *Journal of testing and evaluation*, **26**(2), 1998, pp. 125-131.

[5] Y. Feng, C. Gao, Y. He, T. An, C. Fan and H. Zhang, Investigation on tension–tension fatigue performances and reliability fatigue life of T700/MTM46 composite laminates. *Composite Structures*, **136**, 2016, pp. 64-74.

[6] M.P. Luong, Infrared thermographic scanning of fatigue in metals. *Nuclear Engineering and Design*, **158**(2), 1995, pp. 363-376.

[7] M.P. Luong, Fatigue limit evaluation of metals using an infrared thermographic technique. *Mechanics of materials*, **28**(1), 1998, pp. 155-163.

[8] M.P. Luong. Infrared thermography of fatigue in metals. in *Aerospace Sensing*. International Society for Optics and Photonics, 1992.

[9] M.P. Luong and K.D. Van, Metal fatigue limit evaluation using infrared thermography. *Proceedings of workshop advanced infrared technology and applications, Capri (Italy)*, 1993, pp. 245–253.

[10] J. Montesano, Z. Fawaz and H. Bougherara, Use of infrared thermography to investigate the fatigue behavior of a carbon fiber reinforced polymer composite. *Composite structures*, **97**, 2013, pp. 76-83.

[11] C. Colombo, L. Vergani and M. Burman, Static and fatigue characterisation of new basalt fibre reinforced composites. *Composite structures*, **94**(3), 2012, pp. 1165-1174.

[12] C. Colombo, F. Libonati, F. Pezzani, A. Salerno and L. Vergani, Fatigue behaviour of a GFRP laminate by thermographic measurements. *Procedia Engineering*, **10**(7), 2011, pp. 3518-3527.

[13] M. Karama, Determination of the fatigue limit of a carbon/epoxy composite using thermographic analysis. *Structural Control & Health Monitoring*, **18**(7), 2011, pp. 781-789.

[14] L. Gornet, O. Wesphal, C. Burtin, J.L. Bailleul, P. Rozycki and L. Stainier, Rapid determination of the high cycle fatigue limit curve of carbon fiber epoxy matrix composite laminates by thermography methodology: tests and finite element simulations. *Procedia Engineering*, **66**, 2013, pp. 697-704.

[15] L. Gornet, O. Westphal, P. Rozycki, L. Stainier and G. Kemlin. Rapid determination of the fatigue properties of carbon fiber epoxy matrix composite laminates by self heating tests, *JST-AMAC-Transition statique–dynamique dans les matériaux et structures composites*. 2014.

[16] Z.S. Bagheri, I. El Sawi, H. Bougherara and R. Zdero, Biomechanical fatigue analysis of an advanced new carbon fiber/flax/epoxy plate for bone fracture repair using conventional fatigue tests and thermography. *Journal of the mechanical behavior of biomedical materials*, **35**, 2014, pp. 27-38.

[17] C. Peyrac, T. Jollivet, N. Leray, F. Lefebvre, O. Westphal and L. Gornet, Self-heating method for fatigue limit determination on thermoplastic composites. *Procedia Engineering*, **133**, 2015, pp. 129-135.

[18] R. Attermo and G. Östberg, Measurements of the temperature rise ahead of a fatigue crack. *International Journal of Fracture Mechanics*, **7**(1), 1971, pp. 122-124.

[19] K. Reifsnider and R. Williams, Determination of fatigue-related heat emission in composite materials. *Experimental Mechanics*, **14**(12), 1974, pp. 479-485.

[20] J. Charles, F. Appl and J. Francis, Using the scanning infrared camera in experimental fatigue studies. *Experimental mechanics*, **15**(4), 1975, pp. 133-138.

[21] Q. Guo, X. Guo, J. Fan, R. Syed and C. Wu, An energy method for rapid evaluation of high-cycle fatigue parameters based on intrinsic dissipation. *International Journal of Fatigue*, **80**, 2015, pp. 136-144.

[22] D. Vasiukov, S. Panier and A. Hachemi, Direct method for life prediction of fibre reinforced polymer composites based on kinematic of damage potential. *International Journal of Fatigue*, **70**, 2015, pp. 289-296.

[23] F. Curà, G. Curti and R. Sesana, A new iteration method for the thermographic determination of fatigue limit in steels. *International Journal of Fatigue*, **27**(4), 2005, pp. 453-459.

[24] H. Zhang, G. Wu, Z. Yan, S. Guo, P. Chen and W. Wang, An experimental analysis of fatigue behavior of AZ31B magnesium alloy welded joint based on infrared thermography. *Materials & Design*, **55**, 2014, pp. 785-791.

[25] Q. Guo and X. Guo, Research on high-cycle fatigue behavior of FV520B stainless steel based on intrinsic dissipation. *Acta Metallurgica Sinica*, **90**(4), 2016, pp. 248-255.